12th International Symposium on Turbulence and Shear Flow Phenomena (TSFP12)
Osaka, Japan (Online), July 19-22, 2022

TIME-RESOLVED PIV INVESTIGATION OF GAP RATIO EFFECTS ON TURBULENT FLOW PAST A SQUARE CYLINDER WITH SMOOTH AND ROUGH UPSTREAM WALLS

Heath Chalmers
Department of Mechanical Engineering
University of Manitoba
Winnipeg, MB, R3T 5V6, Canada
chalmerh@myumanitoba.ca

Xingjun Fang
Department of Mechanical Engineering
University of Manitoba
Winnipeg, MB, R3T 5V6, Canada
fangx@myumanitoba.ca

Mark F. Tachie
Department of Mechanical Engineering
University of Manitoba
Winnipeg, MB, R3T 5V6, Canada
mark.tachie@umanitoba.ca

ABSTRACT

Time-resolved particle image velocimetry is used to investigate turbulent flow separation around a square cylinder placed at various gap heights away from a smooth and rough upstream wall. The gap heights range from 0.0 to 2.0 times the cylinder height, while the Reynolds number based on the free-stream velocity and cylinder height is 12 750. The combined effects of gap ratio and wall roughness on the turbulence statistics and coherent structures are analysed. In particular, proper orthogonal decomposition in conjunction with phase averaging are employed to investigate the spatio-temporal characteristics of the vortex shedding motions. The results indicate that the Reynolds stresses are disproportionately high in the upper wake region for smaller gap ratios, but are similar in magnitude to those in the lower wake region at high gap ratios. The vortex shedding motion behind the cylinder is disrupted for gap ratio equal to 0.3 times the step height, particularly when wall roughness is present. The dominant structure behind the surface-mounted cylinder reflects its interaction with coherent structures of the incoming turbulent boundary layer whereas those behind the offset cases are dictated by the vortex shedding motion. Phase averaging shows that wall roughness reduces streamline curvature and increases the Reynolds stress decay rate.

Introduction

Turbulent flow past a square cylinder in the vicinity of a rough wall exhibits distinct and complex flow characteristics such as flow separation, acute streamline curvature, and vortex shedding. Many experimental studies have investigated the effects of turbulence intensity on pressure coefficient and vortex shedding of a square cylinder in uniform flow. The investigation by Saathoff & Melbourne (1999) showed that increasing the turbulence intensity from 5% to 12% decreases the mean pressure coefficient near the leading edge of the cylinder, while a further increase in the turbulence intensity from 12% to 24% increases the mean pressure coefficient. Meanwhile, the vortex shedding structures in the wake region are suppressed for turbulence intensities larger than 20%. An experimental study on near-wall square cylinder by Martinuzzi et al. (2003) showed that the vortex shedding frequency in the wake region is independent of gap ratio, which is at variance with large eddy simulation performed by Samani & Bergstrom (2015).

The flow around a square cylinder becomes more complex when a finite gap is introduced beneath the cylinder due to the interaction between the separated shear layers from either side of the cylinder and the shear layer emanating from the wall. In general, vortex shedding is suppressed when the gap ratio is decreased below a threshold value, nonetheless, the critical gap ratio is not universal but ranges from $G/h = 0.3$ (Martinuzzi et al., 2003) to $G/h = 0.5$ as summarized by Samani & Bergstrom (2015). Samani & Bergstrom (2015) and Shi et al. (2010) showed that the energy content of the low order proper orthogonal decomposition (POD) modes is a function of gap ratio, and the energy of the first two POD modes is reduced when the cylinder is closer to the wall. Shi et al. (2010) also reported relatively poor coherence of the trajectory of the first two POD mode coefficients when the square cylinder is placed near the wall compared to larger gap height cases.

In spite of numerous prior studies, the present understanding of gap ratio effects on the spatio-temporal characteristics of vortical structures around square cylinders is deficient. Furthermore, past studies were performed over smooth walls. Since upstream wall roughness significantly alters the turbulent and unsteady characteristics in forward- backward-facing step flows (Fang & Tachie, 2018), the present study investigates the combined effects of wall roughness and gap ratio on the turbulence statistics and spatio-temporal characteristics of coherent structures around a near-wall square cylinder with upstream wall roughness.

Experimental Procedure

The experiments were conducted in an open recirculating water channel. To investigate the effects of wall roughness on

the flow physics surrounding a square cylinder, two different roughness conditions were employed. For the smooth case, the flow was tripped at the channel inlet using a 100 mm long strip of 16-grit sandpaper. This was followed by a smooth acrylic plate leading up to the square cylinder 3100 mm downstream of the channel inlet. For the rough case, the flow trip consisted of a 100 mm long toothed barrier placed at the channel inlet followed by sandpaper roughness leading up to the cylinder at 4500 mm downstream of the channel inlet. The boundary layer, δ, and momentum, θ, thicknesses, along with the shape factor, δ/θ are shown in Table 1 for the smooth and rough incoming boundary layers. The Reynolds numbers based on the step height and momentum thickness respectively are also shown. The square cylinder had a body height h, of 25 mm and the gap height, G, was varied so that the examined gap ratios G/h were 0.0, 0.3, 0.5, and 2.0.

Table 1. Parameters characterizing the state of the incoming TBLs for different wall conditions.

	Smooth TBL	Rough TBL
U_∞	0.51	0.51
δ/h	3.6	7.2
θ/h	0.46	1.05
H	1.34	1.56
Re_h	12 800	12 800
Re_θ	5 800	13 400

A time-resolved particle image velocimetry (TR-PIV) system was used to measure the velocity field at the mid- span of the test section. $10\mu m$ silver coated hollow glass spheres were used as seeding particles. The seeding particles were illuminated using a dual-cavity dual-head neodymium yttrium lithium fluoride (Nd:YLF) laser emitting green light with a maximum energy of 30 MJ/pulse. Two high-speed complementary metal-oxide semiconductor (CMOS) cameras were used to capture particle images at a frequency of 807 Hz upstream of, over, and downstream of the square cylinder. 48 000 images were taken for the $G/h = 2.0$ case while 60 000 images were collected for the remaining test cases. DaVis version 10 supplied by LaVision Inc. was used to calculate the velocity vectors and an in-house MATLAB script was developed to process the resultant data. The vector calculation of each test case was processed using initial and final interrogation areas of 128 pixel $\times$ 128 pixel with 50% overlap and 24 pixel $\times$ 24 pixel with 75% overlap, respectively.

Results & Discussion

Turbulence Statistics

Figure 1 shows the streamwise Reynolds normal stresses, $\overline{u'u'}$, for the G/h = 0.3 and 2.0 cases, with both the mean streamlines and zero-velocity isopleths superimposed. From the mean streamlines, three distinct recirculation regions are present for each test case, one above the cylinder and one emanating from each of the upper and lower edges of the cylinder in the wake region. The size of the recirculation region is determined using the zero-velocity contour and shortens as the gap ratio increases from G/h = 0.3 to 2.0. This variation is also reported by Shi et al. (2010). However, the present values of mean recirculation length are shorter than those reported previously due to the thicker oncoming turbulent boundary layer along with higher turbulent intensity induced by the upstream rough wall in the present study. Table 2 shows the recirculation length for all test cases investigated. Following the observation from Figure 1, the recirculation length decreases both as the gap size increases, and as a result of upstream wall roughness.

Table 2. Recirculation length, L_r/h, for various test cases.

	L_r/h	
G/h	Smooth Wall	Rough Wall
0.0	10.4	7.8
0.3	2.6	2.1
0.5	1.3	1.7
2.0	0.6	0.7

The contour levels of the $\overline{u'u'}$ show strong turbulence motion in the separated shear layer emanating from the leading edge of the cylinder as well as from trailing edge of the cylinder at both the upper and lower surfaces. The magnitude of the Reynolds stress is larger in the shear layer emanating from the upper edge of the cylinder when the cylinder is placed near the wall. The presence of the wall also introduces a region of strong velocity fluctuations near the wall immediately downstream of the cylinder trailing edge, as shown in Figure 1a. Comparison with the smooth wall data (not shown) reveals that for the G/h = 0.0 and 0.3 cases, the Reynolds stresses are larger over the rough wall but also decay faster in the downstream direction.

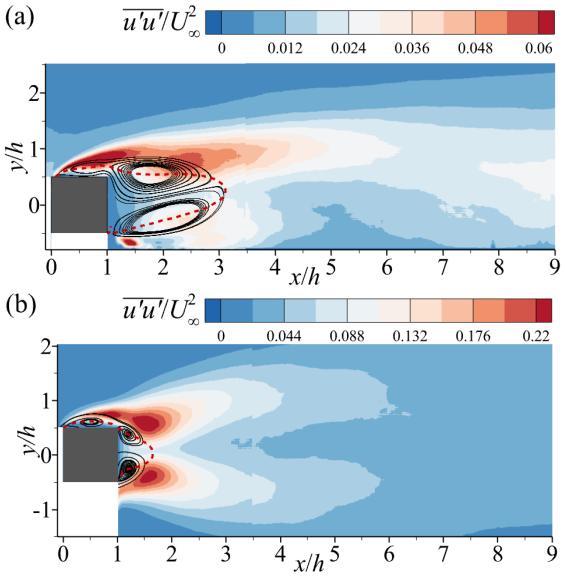

Figure 1. Contours of the $\overline{u'u'}$ Reynolds stresses for the rough wall $G/h = 0.3$ (a) and $G/h = 2.0$ (b) test cases, respectively. The mean streamlines (solid black) and zero-velocity contour (dashed red) are superimposed.

Proper Orthogonal Decomposition

In order to further investigate the spatial characteristics of coherent structures in the cylinder wake, a POD algorithm was implemented according to the snapshot method proposed by Sirovich (1987) wherein a singular value decomposition is performed on the matrix $\psi = V\Lambda M^T$, where the matrices V, Λ, and M represent the POD modes, energy, and coefficients respectively. To show a typical pattern associated with vortex shedding in the wake of a cylinder, Figure 2 displays the first two POD modes for the $G/h = 2.0$ case with a rough upstream wall. The first POD mode shows alternating positive and negative vortices emanating from the upper and lower surfaces of the square cylinder. The second POD mode shows similar structures as the first POD mode, but with a downstream shift of approximately 1.5 step heights. Furthermore, the first two POD modes of this test case contribute 56.2% of the total POD energy. These observation are in accordance with a POD mode pair as defined by Riches et al. (2018) for vortex shedding in the wake of a cylinder.

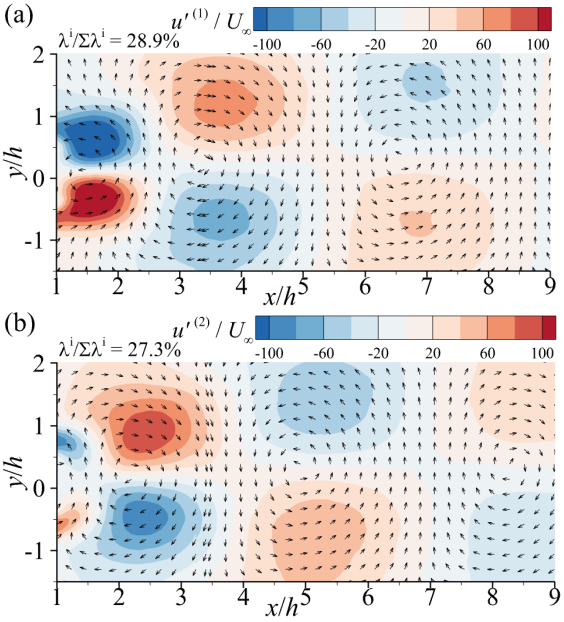

Figure 2. Contours of the first two POD modes for the rough wall $G/h = 2.0$ test case.

Figures 3 and 4 show the POD mode contours for the $G/h = 0.3$ case with smooth and rough upstream wall respectively. For the smooth case, alternating positive and negative vortices are observed in both POD modes, however a significant incline of vortices away from the wall is noticeable. Also, the downstream shift of coherent structures from the first mode to the second mode is less than one step height. The rough case exhibits markedly different behaviour. Within the first POD mode, multiple vortices are clustered near the bottom wall, whereas the second POD mode exhibits two large vortices centred at the body centerline downstream of the cylinder. These observations deviate from the traditional understanding that von Karman vortices present themselves in the first two POD modes (Samani Bergstrom, 2015; Shi et al., 2010). These results suggest that upstream wall roughness significantly modifies the vortical structures downstream of the gap exit near the wall, and therefore, disturbs the occurrence of organized vortex shedding motion.

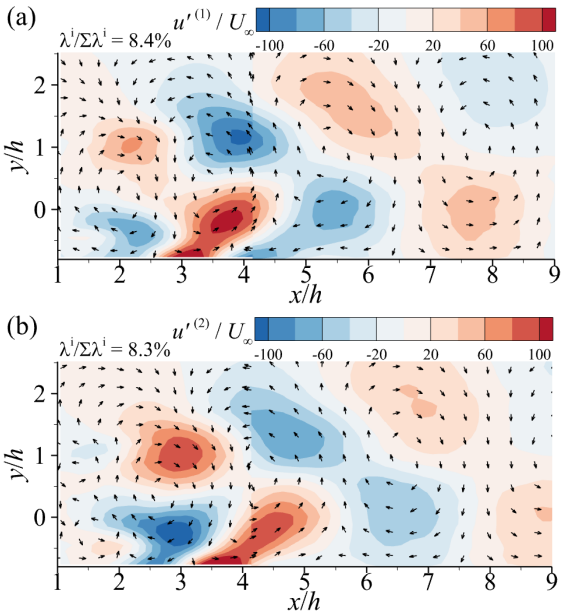

Figure 3. Contours of the first two POD modes for the smooth wall $G/h = 0.3$ test case.

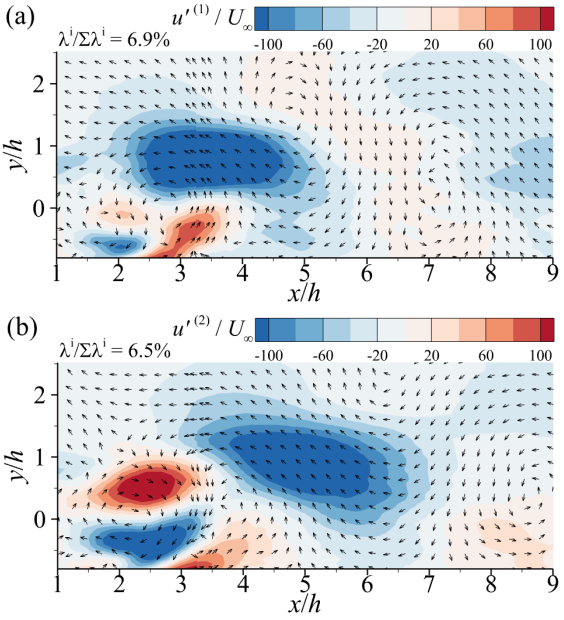

Figure 4. Contours of the first two POD modes for the rough wall $G/h = 0.3$ test case.

Several researchers have used phase portraits of the first two POD mode to visualize the coherence of the vortex shedding motions in the wake of an offset cylinder (Shi et al. 2010; Riches et al. 2018). In this same vain, Figure 5 compares the temporal trajectory of the first two POD mode coefficients for the rough wall $G/h = 0.3$ and the smooth wall $G/h = 0.5$ cases. The orbital trajectory is discernible to varying degrees for all test cases indicating the occurrence of vortex shedding motions in each case. Evidently, the orbital is more organized for the larger gap ratio and smooth wall cases. This is indicative of weaker perturbation of incoming turbulence on the vortex shedding motion when the cylinder is farther away from the wall especially for the upstream smooth wall case. In particular, for the rough wall $G/h = 0.3$ case, the trajectory of the first

two POD mode coefficients is the most random compared with other cases. This randomness is attributed to the intermittency of vortex shedding motion imposed by the significant incoming turbulence through the gap. Bai & Alam (2018) and Bailey et al. (2002) observed that for a square cylinder, the regular vortex shedding motion is interrupted as the shear layer intermittently reattaches on the side surfaces. The intermittency of vortex shedding observed in Figure 5 is likely due to a strong tendency of the mean flow to reattach on the undersurface of the cylinder due to the high incoming turbulence intensity.

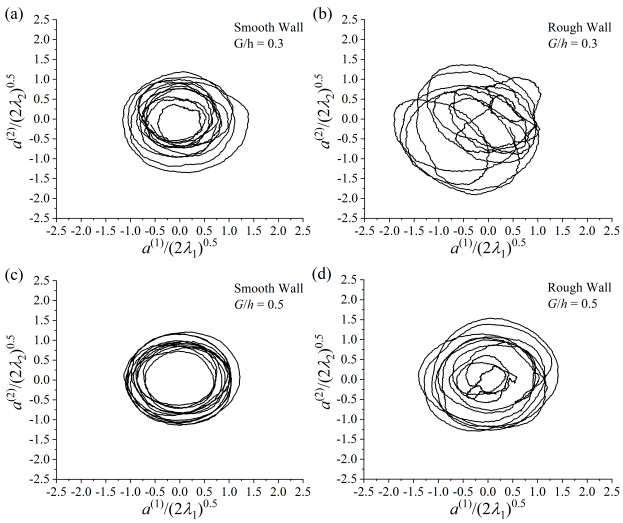

Figure 5. Phase portraits of the first two POD mode coefficients for the $G/h = 0.3$ (a,b) and $G/h = 0.5$ (c,d) test cases.

In order to investigate the effects causing the overall dampening of vortex shedding at smaller gap ratios, the frequency spectra of the first two POD mode coefficients are presented in Figure 6 along with the spectra of the velocity fluctuations at the cylinder centerline in the upstream turbulent boundary layer. For the surface-mounted cylinders, the first two POD mode oscillate at low frequencies between $St = 0.02$ and $St = 0.03$ which is similar to that of the incoming flow conditions. Once the cylinder is offset from the wall, the two mode coefficients possess identical dominant frequencies for each test case, that is distinct from the boundary layer frequency. In general, the dominant frequency of vortex shedding motions behind a square cylinder are reported to be between $St = 0.129$ and $St = 0.140$ (Durao et al. 1991; Bosch et al. 1996; Kumeran & Vengadesan 2007). This range is consistent with the dominant frequency for the smooth wall $G/h = 0.5$ case, however the other test cases possess lower dominant frequencies. Based on the results shown in Figure 6, the dominant frequency becomes smaller with both smaller gap ratios and increased turbulence intensity as a result of wall roughness. Overall, it is concluded that the dominant structure for the wall-mounted cylinder case is dictated by the coherent structures embedded in the incoming flow condition. However, the vortex shedding motion behind an offset cylinder overwhelms the perturbation of incoming turbulence.

Phase Averaging

A phase angle, $\phi = tan^{-1}\left(\frac{a^{(2)}\sqrt{\lambda_1}}{a^{(1)}\sqrt{\lambda_2}}\right)$, is defined using the trajectory map of the first two POD mode coefficients in

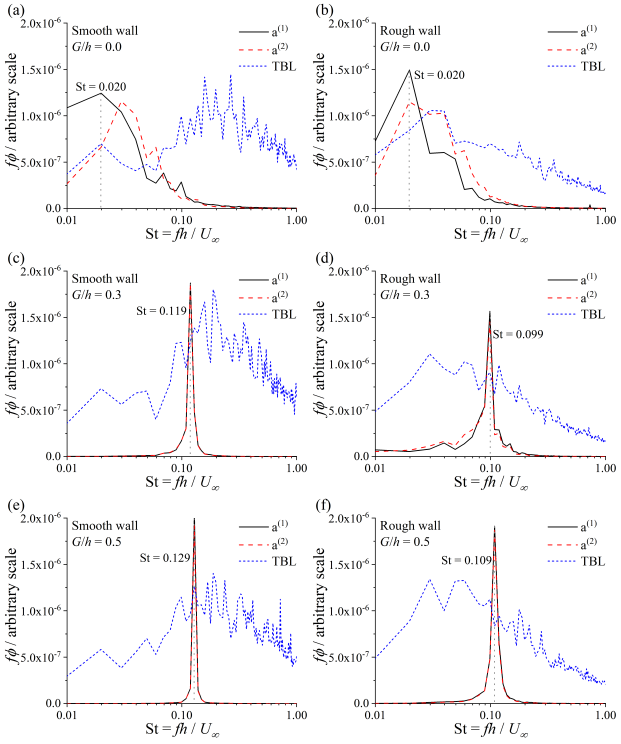

Figure 6. Frequency spectra of the first two POD mode coefficients and the velocity fluctuations at the step height in the corresponding turbulent boundary layer for the $G/h = 0.0$ (a,b), $G/h = 0.3$ (c,d), and $G/h = 0.5$ (e,f) test cases.

Figure 5 to perform phase averaging of the flow field. Figures 7 and 8 show the phase-averaged streamwise Reynolds normal stress, $\langle u'u' \rangle$, at three different phase ranges for the smooth and rough $G/h = 0.3$ cases respectively. The phase averaged streamlines provide insight into the unsteady oscillations of the turbulent recirculation region and is reminiscent of the unsteady recirculation described by Sherry et al. (2010) over a forward-facing step using phase averaging. In accordance with the results from Table 2, the streamwise extent of the recirculation bubble is larger for smooth wall case in Figure 7 than in the rough wall case shown in Figure 8. Furthermore, the height of the recirculation bubble above the cylinder is higher in the smooth wall case than the rough wall case. This indicates that wall roughness decreases the vertical amplitude at which the wake oscillates behind a square cylinder, and reduces the intensity of streamline curvature in the wake. These observations are in accordance with the findings of Shi et al. (2010). The same modulation of the wake is not observed below the square cylinder due to wall confinement effects. Figure 7 further reveals that at specific phase angles, a third recirculation bubble exists downstream of the cylinder near $x/h = 4.0$. This additional recirculation bubble is suppressed when wall roughness is introduced upstream of the cylinder.

The progression of the phase-averaged Reynolds stresses through different phase bins depicts the downstream convection of recirculation bubbles. Recirculation regions originating over the step are convected forwards and dissipate in the downstream direction. Shi et al. (2010) also showed that as the recirculation bubbles are convected downstream, regions of low-momentum fluid near the gap exit are carried downstream as well. During this process, patches of elevated Reynolds

stresses that originate in the upper and lower shear layers are also convected downstream. Compared with the smooth case shown in Figure 7, these patches of $\langle u'u' \rangle$ in the rough wall case generally decay faster and possess stronger magnitudes in the upper shear layer. This is why the elevated time averaged Reynolds normal stress extends further in the downstream direction, and has a smaller magnitude in the upper shear layer with an upstream smooth wall. Furthermore, the peak $\langle u'u' \rangle$ is found along the separating streamlines which is in god agreement with both Sherry et al. (2010) and Shi et al. (2010).

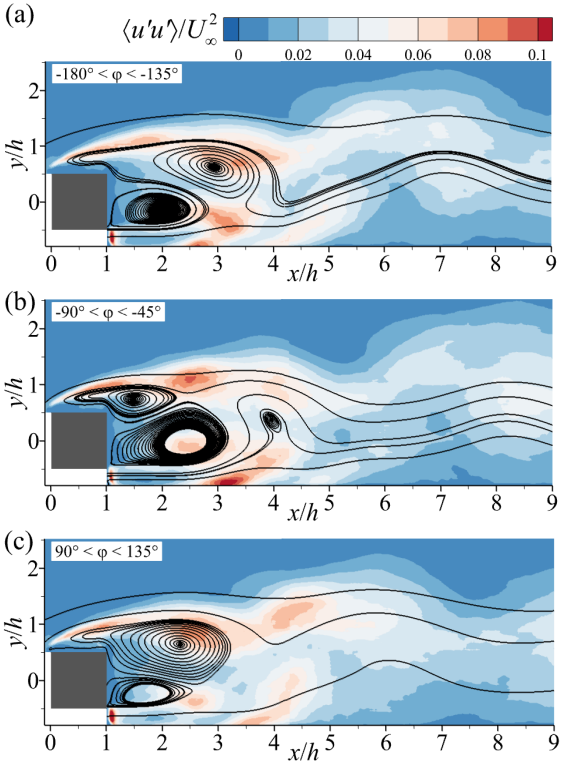

Figure 7. Phase-averaged streamwise Reynolds normal stress, $\langle u'u' \rangle$, for the smooth wall $G/h = 0.3$ case at three different phase bins.

Conclusions

Turbulent flows past square cylinders offset from a wall at different distances were studied using time-resolved particle image velocimetry. The examined ratios of the gap height underneath the cylinder to cylinder height were 0.0, 0.3, 0.5, and 2.0. Two upstream roughness conditions were employed to investigate wall roughness effects on the mean flow, Reynolds stresses, and vortex shedding phenomenon in the cylinder wake.

There exists two counter-rotating recirculation bubbles in the wake of offset cylinders, while only one reverse flow region exists behind a wall-mounted cylinder. The streamwise extent of the recirculation bubbles decreases when there is wall roughness present and at smaller gap ratios. The streamwise decay rate of Reynolds stresses increases with gap ratio. Furthermore, the magnitudes of Reynolds stresses are larger in the upper recirculation region when the gap ratio is equal to 0.3 times the step height, but is similar to that in the lower recirculation region when the gap size is increased to 2.0 times the step height.

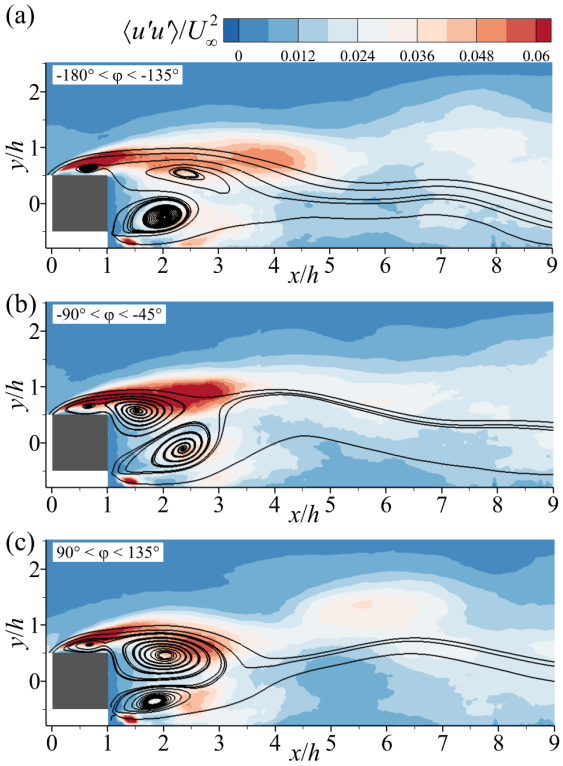

Figure 8. Phase-averaged streamwise Reynolds normal stress, $\langle u'u' \rangle$, for the rough wall $G/h = 0.3$ case at three different phase bins.

A proper orthogonal decomposition (POD) was performed to investigate the coherent structures in the wake region. Notably, the contribution of the first two POD modes to the total energy decreases significantly at smaller gap ratios. This suggests that the coherence of vortical structures in the wake region decreases at smaller gap ratios and with wall roughness. This observation is also noted in the phase portraits of the first two POD modes, showing that proximity to the wall and wall roughness both act to disrupt vortex shedding motions in the wake. Additionally, analysis of the frequency spectra shows that for the wall-mounted case, the fluctuation of the first POD mode coefficient reflects the interaction of the cylinder with the incoming flow structures. For the offset cylinders, on the other hand, the first two mode coefficients possess identical dominant frequencies that are significantly higher than the dominant frequency of the turbulent boundary layer, and represent the vortex shedding motions in the wake region.

Phase averaging reveals that both mean recirculation bubbles and patches of elevated Reynolds stresses are convected downstream through time. Furthermore, the temporal variation of the streamlines shows that wall roughness acts to diminish the intensity of streamline curvature and also increases the streamwise decay rate of Reynolds stresses in the wake.

REFERENCES

Bai, H., & Alam, M.M., 2018, 'Dependence of Square Cylinder Wake on Reynolds Number', *Phys. Fluids*, Vol. 30, pp. 015102.

Bailey, S.C.C., Kopp, G.A., & Martinuzzi, R.J., 2002, 'Vortex Shedding from a Square Cylinder Near a Wall', *J. Turb.*, Vol. 3, pp. N3.

Bosch, G., Kappler, M., Rodi, W., 1996, 'Experiments on the Flow Past a Square Cylinder Placed Near a Wall', *Exp. Thermal Fluid Science*, Vol. 13, pp. 292-305.

Durao, D.F.G., Gouveia, P.S.T., Pereira, J.C.F., 1991, 'Velocity Characteristics of the Flow Around a Square Cross Section Cylinder Placed Near a Channel Wall', *Exp. Fluids*, Vol. 11, pp. 341-350.

Fang, X., Tachie, M.F., 2019, 'Unsteady Characteristics of Turbulent Separations Over a Forward-Backward-Facing Step', *J. Fluid Mech.*, Vol. 863, pp. 994-1030.

Kumeran, M., Vengadesan, S., 2007, 'Flow Characteristics Behind Rectangular Cylinder Placed Near a Wall', *Num. Heat Trans. Part A*, Vol. 52, pp. 643-660.

Martinuzzi, R.J., Bailey, S.C.C., Kopp, G.A., 2003, 'Influence of Wall Proximity on Vortex Shedding from a Square Cylinder', *Exp. Fluids*, Vol. 34, pp. 585-596.

Riches, G., Martinuzzi, R., Morton, C., 2018, 'Proper Orthogonal Decomposition Analysis of a Circular Cylinder Undergoing Vortex-Induced Vibrations', *Phys. Fluids*, Vol. 30, pp. 105103.

Saathoff, P., Melbourne W.H., 1999, 'Effects of Freestream Turbulence on Streamwise Pressure Measured on a Square-Section Cylinder', *J. Wind Eng. Ind. Aero.*, Vol. 79, pp. 61-78.

Samani, M., Bergstrom, D.J., 2015, 'Effect of a Wall on the Wake Dynamics of an Infinite Square Cylinder', *Intl. J. Heat Fluid Flow*, Vol. 55, pp. 158-166.

Sherry, M., Lo Jacono, D., Sheridan, J., 2010, 'An Experimental Investigation of the Recirculation Zone Formed Downstream of a Forward Facing Step', *J. Wind Eng. Ind. Aero.*, Vol. 98, pp. 888-894.

Shi, L.L., Liu, Y.Z., Wan, J.J., 2010, 'Influence of Wall Proximity on Characteristics of Wake Behind a Square Cylinder: PIV Measurements and POD Analysis', *Exp. Thermal Fluid Science*, Vol. 34, pp. 28-36.

Sirovich, L., 1987, 'Turbulence and the Dynamics of Coherent Structures. Parts I, II, and III', *Quart. App. Math.*, Vol. 45 (561-571), pp. 573-590.